RESEARCH ARTICLE

Radioimmunoimaging with Mixed Monoclonal Antibodies of Nude Mice Bearing Human Lung Adenocarcinoma Xenografts

Dong Duan[1]*, Shao-Lin Li[2], Yu-Quan Zhu[1], Tao Zhang[3], Cheng-Ming Lei[1], Xiang-Hua Cheng[1]

Abstract

The present study was conducted to evaluate radioimmunoimaging (RII) and in vivo distribution of mixed antibodies ^{99m}Tc-EGFR-mAb and ^{99m}Tc-CD44- mAb in nude mice bearing human lung adenocarcinoma xenografts. Single and mixed applications of the two radiolabeled monoclonal antibodies (mAbs) were compared. Direct labeling of ^{99m}Tc was applied to radiolabel the EGFR and CD44 mAbs. The properties of the radiolabeled antibodies were then characterized. RII and assessment of the distribution of the antibodies in nude mice bearing lung adenocarcinoma xenografts were achieved by applying separate and combined doses of ^{99m}Tc-EGFR-mAb and ^{99m}Tc-CD44-mAb. The labeling rates of ^{99m}Tc for EGFR-mAb and CD44-mAb were 91.5% ± 3.8% and 92.3% ± 4.1% respectively, with specific activities of 2.8 and 2.9 MBq/μg, respectively, and radiochemical purities (RCP) of 96.5% and 96.2%. The radioactivity uptake of the combined application of both radiolabeled antibodies was clearly higher than with a single application of either alone. The relative values of target-to-nontarget (T/NT) measured through the regional interest (ROI) technique were 5.59 ± 0.42 (mixed antibodies), 2.78 ± 0.20 (^{99m}Tc-EGFR-mAb), and 2.28 ± 0.16 (^{99m}Tc-CD44-mAb) in the RII. The body distribution of the radiolabeled antibodies and their imaging results were basically identical. Application of the mixed antibodies with ^{99m}Tc-EGFR-mAb and ^{99m}Tc-CD44-mAb can increase the radioactivity uptake of tumor tissue, leading to more ideal target-to-nontarget ratios, and therefore superior results.

Keywords: EGFR - CD44 - radioimmunoimaging - molecular imaging - monoclonal antibody

Asian Pacific J Cancer Prev, **13 (9)**, 4255-4261

Introduction

Lung cancer is currently one of the most common malignancies with high global morbidity and mortality (Rom et al., 2000; Tachfouti et al., 2012). The incidence and mortality rates of lung cancer in China have rapidly increased. Lung cancer has emerged as the leading cause of cancer deaths in China's urban population. The World Health Organization (WHO) predicted that China will have the largest lung cancer population in the 21st century (Lopez, 1998). The clinical diagnosis for lung cancer currently relies mainly on imaging methods (e.g., chest radiography, computer tomography), magnetic resonance imaging, and positron emission computed tomography, cellular pathology by examining sputum exfoliated cancer cells, and histological techniques such as biopsy. Although these traditional diagnostic methods have been used for many years in clinical practice, these techniques sometimes lack adequate sensitivity and specificity, especially during the early stages of lung cancer. According to statistics, the five-year survival rate of lung cancer patients is still only 10% to 15%. The main reason for this low survival rate is that most lung cancer patients are diagnosed in the advanced stages, during which the optimal time for treatment is lost, resulting in a significant increase in mortality (Greenlee et al., 2000; Granville and Dennis, 2005). Hence, the early diagnosis and treatment of lung cancer have attracted the concern and attention of an increasing number of clinicians all over the world, especially in developed countries (Bellomi et al., 2006; Neal et al., 2007).

Cancer RII is a type of molecular nuclear medicine imaging that applies specific antibodies of tumor-specific expressed antigens labeled with radionuclides for imaging. This technique combines the high specificity of antibody antigens with the high sensitivity of nuclear medicine imaging. The development of monoclonal antibodies (mAbs) has accelerated the development of RII, which is at present a very useful tool in the localized and qualitative diagnosis of cancer, especially during the early stages (Boswell and Brechbiel, 2007; Smith-Jones et al., 2008). RII has obtained favorable success in recent years with many kinds of tumors, such as in hepatic and gastrointestinal tumors as well as lymphoma. Many RII

*[1]Department of Nuclear Medicine, [3]Departments of Oncology, the First Affiliated Hospital of Chongqing Medical University, [2]Departments of Nuclear Medicine, the Basic Medicine of Chongqing Medical University, Chongqing, China *For correspondence: duand26@yahoo.com.cn*

imaging agent kits are used in the market today (Shi et al., 1997; Gmeiner Stopar et al., 2008; Artiko et al., 2011).

The lack of tumor specific antigens and weak antigenicity or heterogeneity of the tumor-specific antigens may be the main barriers for lung cancer RII and other tumors. Finding tumor-specific high expression antigens and methods to increase the uptake of radioactivity at the tumor site is the key to the development of lung cancer RII. Some studies have demonstrated that the application of mixed labeled antibodies to one type of cancer (called "antibody cocktail") may be an ideal methods to increase the radioactivity uptake in the tumor site (Hay et al., 2002; Petronzelli et al., 2005).

Epidermal growth factor receptor [EGFR] and CD44 are two kinds of transmenbrane protein. Many studies (Cichy et al., 2005; Malle et al., 2005; Gao et al., 2007; Sartori et al., 2007; Eren et al., 2008; Fukui and Hirsch et al., 2008; Ikeda et al., 2008; Mitsudomi, 2008; Jin et al., 2011) have found overexpressions of these two transmembrane proteins in lung adenocarcinoma and these proteins play important roles in facilitating the proliferation, invasion, metastasis, and apoptosis of lung cancer cells. In the present study, two types of transmembrane proteins (EGFR and CD44) were selected as the target antigens of lung adenocarcinoma. RII was performed on the mAb by single and mixed applications to evaluate the reliability of these two proteins as target antigens of lung cancer and determine the effect of a mixed application of the two antibodies in increasing the radioactivity uptake for RII.

Materials and Methods

Cell and animal models

Human lung adenocarcinoma cells A549 were provided by the Department of Pathophysiology of Chongqing Medical University. The cells were used in the exponential phase of growth. The Animal Center of Chongqing Medical University provided 120 four-week-old female nude mice weighing 15 g to 20 g. A cell suspension (1.0×10^8/ mL) was made with PBS. The mice were injected with 1.0×10^7/0.1 mL suspension in the lateral side of the forelimbs. The survival of the nude mice and the formation of the subcutaneously implanted tumors were observed for approximately 3 wk to 4 wk. This study was carried out in strict accordance with the recommendations in the Guide for the Care and Use of Laboratory Animals of the National Institutes of Health. The animal use protocol has been reviewed and approved by the Institutional Animal Care and Use Committee (IACUC) of Chongqing Medical University.

Labeling of mAb

The direct labeling method for ^{99m}Tc was applied to the two mAbs (100 μg): anti-EGFR mAb (No: GR15L), anti-CD44 mAb (No: 217594, Merck, Merck German) (Fritzberg et al., 1988). Reagents of purified and freeze-dried EGFR and CD44 mAbs (5 mg each) were dissolved in 1 mL normal physiological saline (NS). The reagents were filled with nitrogen gas for 5 min. The reducing agent 2-mercaptoethanol (2-ME) was added in a molar ratio 2-ME: antibody = 2000:1. After having been fully shaken, the reagent was set under ambient temperature for 30 min. The reduced antibodies were placed into a SephadexG 50 Gel micro-centrifugal column for centrifugation (2000 r/min, twice, 5 min each time). The column had been washed by buffer solution and dried by centrifugation. The excess 2-ME was removed, and 0.02 mol/L phosphate-buffered saline (PBS) (pH7.4) was applied to the elution. The protein concentration was determined by spectrophotometric determination at 280 nm. A total of 2 mL NS was used to dissolve two methylene diphosphonate (MDP) kits, each containing 5 mg MDP and 0.5 mg SnCl2·2H2O. A total of 40 μL MDP reagent and 300 MBq ^{99m}TcO4- eluent with a specific radioactivity of 1.11 GBq/mL were added to two doses of 200 μL purified and reduced antibodies, respectively. After 20 min of intensive mixing and reaction under full shaking, radiolabeling of the mAbs was performed.

Purification of radiolabeled antibodies

The two aforementioned radiolabeling reaction solutions were applied to a 1 cm × 15 cm Sephadex G50 column. For elution, 0.01 mol/L PBS was used at a flow rate of 8 drops/min. A total of 150 tubes (6 drops /tube) of eluent were collected. The counts per minute (cpm) of each tube were measured by a γ-counter (SN-6930B, Shanghai, China). The eluting curve of each labeled antibody was subsequently obtained. The eluent that represents the first radioactive peak of each curve was collected, and the purified radiolabeled antibodies were obtained.

Determination of physical properties

After the purification of the labeled antibodies by Sephadex G50 column, the purified antibodies were collected, and the labeling rates were calculated by the following formula: radioactivity of purified antibodies (cpm)/total radioactivity of labeling reaction solutions (cpm) ×100%. Then silica gel thin-layer chromatography (TLC) was performed to measure the radiochemical purity. Two kinds of development systems were applied in the study: developing agent A was composed of 10% trichloroacetic acid, whereas developing agent B was composed of ethanol, ammonia water, and water (concentration ratio = 2:1:5). A total of 10 μl labeling reaction solution was drawn out on 2 cm × 18 cm TLC-SG chromatographic paper (2 cm from base line). The migration length of the developing agent was 10 cm. TLC paper was air-dried at the end of the chromatography and cut into 1 cm pieces. The radioactivity of each piece of chromatographic paper was measured by the γ-counter. We calculate the RCP as the following formula: radioactivity of labeled antibodies after chromatographic (cpm)/total radioactivity of purified labeled antibodies before chromatographic×100%. Finally, we calculated the specific activity of the labeled antibodies by the following formula: radioactivity of labeled antibodies (MBq) ×RCP/ quality of the labeled antibodies (μg) and of each labeled antibody were calculated.

Determination of stability of the radiolabeled antibodies

Two samples were drawn from each purified

radiolabeled antibody (500 μL for each sample). One sample was placed at room temperature for 1, 6, 12, and 24 h. The other sample was mixed with twice its volume of fresh human serum and incubated at 37 °C for 0.5, 1, 2, 4 and 24 h. The RCP was measured by ITLC at each time point. In vitro and in vivo stabilities of the radiolabeled antibodies were evaluated by observing variations in RCP.

Identification of immunoreactivity of the radiolabeled antibodies

The immunofluorescence technique was applied in the identification of the immunoreactivity of the radiolabeled antibodies. First, A549 was fixed on a glass slide on which the radiolabeled antibodies were then dropped. Then, the second fluorescent antibodies (FITC-Goat Anti-Mouse IgG, Shanghai, China) were also dropped on the glass slide. The antibody was then observed and counted under a fluorescence microscope. The percentage of the radiolabeled antibodies' binding tumor cell was acquired by fluorescent automatic cell counter (Digital Bio Technology, Korea). An immunofluorescence picture was taken and compared with that of the antibodies before labeling.

RII and in vivo distribution of radiolabeled antibodies

A total of 120 nude mice bearing human A549 xenografts were divided randomly into A, B, and C groups (40 mice in each group). Freshly prepared radiolabeled antibodies were injected into the mice via the tail vein. Group A was injected with 0.5 mL ^{99m}Tc-EGFR-mAb. Group B was injected with 0.5 mL ^{99m}Tc-CD44-mAb. Group C was injected with a combined 0.25 mL ^{99m}Tc-EGFR-mAb and 0.25 mL ^{99m}Tc-CD44-mAb. The radioactivity of the radiolabeled antibodies injected into each nude mouse was in the range of 9.25 MBq to 11.1 MBq.

Planar RII was performed at 2, 4, 8, 16, and 24 h post-injection using a γ-camera (Siemens, Germany, Symbia T2). Six mice were selected randomly for imaging. A high-resolution low-energy pinhole collimator (128 × 128 matrix and 4.8 mm pixel size) was used. The ^{99m}Tc window was centered at 140 keV and had 15% width (range = 129.5 keV to 150.5 keV) and 2× magnification. The acquisition time for each frame was 2 min to 3 min (mean radioactive count = 25000 ± 3000). Finally, the T/NT ratios (radioactive count of the tumor site was compared with that of the contralateral corresponding site) of each phase were calculated by the ROI technique. After 2, 4, 8, 16, and 24 h post-injection of the radiolabeled antibodies, six randomly selected nude mice in each group were sacrificed by cutting their necks at each time point. Blood was collected by retro-orbital bleeding and placed into previously weighed tubes. The hearts, livers, spleens, lungs, stomachs, kidneys, intestines, skeletons, brains, and tumor tissues were removed, placed on filter paper for blood blotting, and placed into tubes that had been weighed separately. The radioactive counts per minute (cpm) of each tissue were measured immediately, and the cpm of the standard source was measured simultaneously each time. The weight of each tissue and its uptake rate was measured. We used ID%/g to represent the uptake rate (ID %/g = radioactive count of tissue / weight of issue / standard source counting × 100%). Meanwhile, the tumor/blood (T/B) and tumor/muscle (T/M) ratios of each labeled antibody in the bodies of each group of nude mice were calculated and compared.

Statistical analysis

Mean values (mean ± SD) between the groups were compared using the Student's unpaired two-tailed t-test. All statistical tests were two-sided, and differences were considered significant when $p < 0.05$. Statistical analysis was performed using SPSS 11.5 statistical software.

Results

All nude mice survived. Single subcutaneously implanted tumors formed in each mouse 3 wk post-injection of A549 cells. The diameter of the tumor was approximately 0.7 cm to 1.0 cm. There were no swellings or ulcerations at the injection spots.

The eluting curve of each radiolabeled antibody is shown in Figure 1. We collected the first radiation peak of each antibody. Purified ^{99m}Tc-EGFR-mAb and ^{99m}Tc-CD44-mAb were obtained.

Physical properties of radiolabeled antibodies

The labeling rates of ^{99m}Tc for EGFR-mAb and CD44-mAb were 91.8% ± 3.6% and 92.1% ± 3.8%, respectively, which were calculated as the formula mentioned above. The RCP of ^{99m}Tc-EGFR-mAb and ^{99m}Tc-CD44-mAb were 96.3% ± 3.4% and 95.8% ± 3.3% respectively obtained by analysis of TLC. And the specific activities of these two labeled antibodies calculated by the formula were 3.0 MBq/μg ± 0.3 MBq/μg (^{99m}Tc-EGFR-mAb) and 2.9 MBq/μg ± 0.2 MBq/μg (^{99m}Tc-CD44-mAb), respectively.

Stability of radiolabeled antibodies

As shown in Table 1, the RCPs of the two antibodies were more than 90% after they were placed at room temperature for 6 h. The RCPs evidently decreased after 24 h, but were still more than 86%. Table 2 shows a slight decline in the RCPs of both radiolabeled antibodies. However, the RCPs were still over 88% 4 h post-incubation with twice the volume of fresh human serum at 37 °C. These results indicate that the two purified labeled antibodies exhibit good stability in vitro and in vivo.

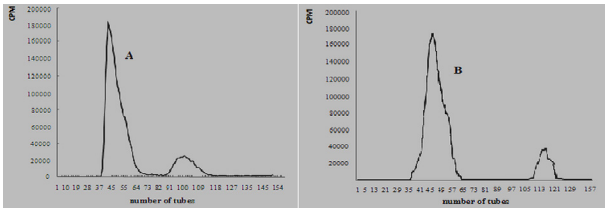

Figure 1. Elution Curve of Labeled Antibodies (A: 99mTc-EGFR-mAb, B: 99mTc-CD44-mAb)

Table 1. Changes in RCP of Labeled Antibodies at Room Temperature Over Time (%, Mean±SD, n=5)

	1h	6h	12h	24h
^{99m}Tc-EGFR-mAb	96.1±3.5	92.8±3.8	89.6±2.9	86.6±3.0
^{99m}Tc-CD44-mAb	95.9±3.3	93.0±3.2	88.9±3.0	86.5±2.8

Table 2. Change of RCP of Labeled Antibodies After Incubating with 2 Times Volume of Fresh Human Serum at 37 °C (%, Mean±SD, n=5)

	0.5h	1h	2h	4h
^{99m}Tc-EGFR-McAb	96.3±3.3	93.4±3.1	90.8±2.8	88.9±2.5
^{99m}Tc-CD44-McAb	96.5±3.1	93.2±3.5	90.6±2.6	89.1±2.6

Table 3. In Vivo Distribution of Mixed mAb in Tumor-Bearing Nude Mice (%ID/g, mean ± SD, n=6)

	2h	4h	8h	16h	24h
Tumor	5.28±1.75	6.88±1.92	10.26±3.21	15.50±4.45[a]	11.87±3.36
Blood	5.86±2.10	5.10±1.98	4.65±1.82	3.01±1.31	2.82±1.16
Heart	4.98±2.53	3.11±2.01	2.13±1.26	1.50±0.92	1.15±0.48
Liver	7.98±3.51	6.56±2.81	5.09±2.21	4.31±1.56	3.20±1.10
Spleen	8.31±3.64	6.72±2.53	5.15±2.28	4.56±1.60	3.18±1.06
Lung	4.76±2.41	3.28±1.65	2.01±1.02	1.47±0.52	1.08±0.51
Kidney	6.65±2.82	9.88±3.82	7.33±2.91	4.46±2.32	2.81±1.21
Stomach	1.68±0.61	1.52±0.45	1.28±0.29	0.99±0.22	0.78±0.15
Bowel	1.51±0.44	1.33±0.32	1.20±0.28	0.95±0.16	0.69±0.11
Muscle	1.18±0.21	1.06±0.13	0.92±0.10	0.65±0.06	0.59±0.05
Bone	1.06±0.19	1.00±0.12	0.86±0.8	0.57±0.06	0.52±0.05
Brain	0.85±0.11	0.81±0.08	0.73±0.06	0.64±0.05	0.42±0.03

Note: [a]: $p < 0.05$ (compared to other four time point)

Table 4. In Vivo Distribution of ^{99m}Tc-EGFR-mAb in Tumor-bearing Nude Mice (%ID/g, Mean ± SD, n=6)

	2h	4h	8h	16h	24h
Tumor	4.68±1.65	5.65±1.98	7.96±2.43	12.50±3.56[b]	9.21±3.21
Blood	6.21±2.25	5.15±2.01	4.85±1.98	3.52±1.61	2.72±1.25
Heart	5.21±2.85	3.22±2.21	2.01±1.56	1.65±0.98	1.21±0.52
Liver	9.86±3.68	7.02±3.02	5.56±2.25	4.12±1.68	3.65±1.12
Spleen	10.01±3.88	6.65±2.91	5.02±2.21	4.35±1.96	3.18±1.21
Lung	5.12±2.42	3.62±2.34	2.16±1.12	1.63±0.62	1.18±0.48
Kidney	6.05±3.01	11.21±3.99	5.05±2.65	3.32±1.20	2.98±0.96
Stomach	1.65±0.51	1.44±0.46	1.22±0.31	0.99±0.22	0.78±0.16
Bowel	1.42±0.38	1.31±0.35	1.12±0.21	0.91±0.18	0.69±0.11
Muscle	1.21±0.23	1.08±0.16	0.98±0.11	0.76±0.09	0.63±0.06
Bone	1.11±0.18	0.95±0.13	0.89±0.11	0.72±0.09	0.51±0.06
Brain	0.96±0.12	0.78±0.09	0.65±0.06	0.58±0.05	0.42±0.03

Note: [b]: $p < 0.05$ (compared to other four time point)

Immunoreactivity of radiolabeled antibodies

The immunofluorescence method was applied to detect the immunoreactivity of ^{99m}Tc-EGFR-mAb and ^{99m}Tc-CD44-mAb. The immunofluorescence photos of two mAb before and after labeling were shown in Figure 2. The immunoreactivity of the antibodies, counted by a fluorescence automatic cell counter, were 58.5% and 56.2%, respectively, prior to the radiolabeling of the antibodies. These values slightly decreased to 57.6% and 55.8%, respectively post-radiolabeling of the antibodies. These results show that there was no significant decline in the immunoreactivity of the two antibodies after radiolabeling.

RII for single or mixed radiolabeled antibodies

Planar γ-camera imaging for the three groups (six mice in each group) of nude mice bearing human lung adenocarcinoma xenografts was conducted 2, 4, 8, 16, and 24 h post- injection of the radiolabeled antibodies. According to the images of each group of nude mice at each time point, the imaging agent did not accumulate evidently in the tumor location during the early stage (2 h),

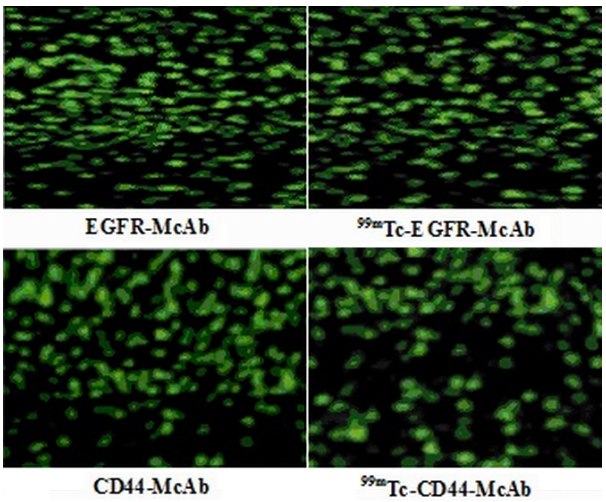

Figure 2. Immunofluorescence Photo of Two mAb Before (Left Panel) and After Labeling (Right Panel)

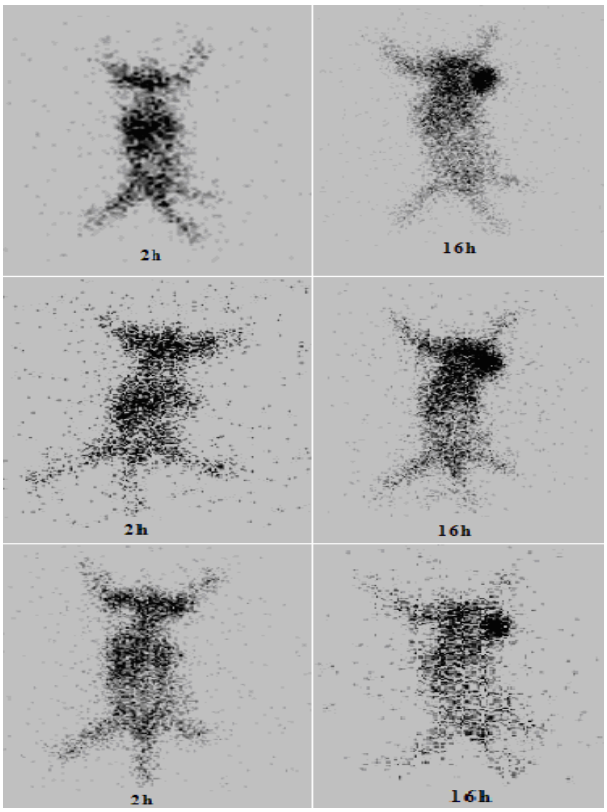

Figure 3. RII Images (2h and 16h) of Partial Animal Model with Different Labeled Antibodies (First row: mixed antibodies, second row: 99mTc-EGFR-mAb, third row: 99mTc-CD44-mAb)

but the blood, liver, and spleen exhibited a high radioactive background. With time, the uptake of the imaging agent in the tumor increased gradually, while that in liver and spleen as well as blood declined gradually. The maximum uptake in the tumor appeared at 16 h with imaging (especially evident in the group with mixed antibodies). RII images (at 2 and 16 h) of the partial animal model with different radiolabeled antibodies are shown in Fig. 3. In the 16 h images of the three groups (^{99m}Tc-EGFR-mAb, ^{99m}Tc-CD44-mAb, and mixed antibodies), the T/NT were 2.78 ± 0.20, 2.28 ± 0.16 and 5.59 ± 0.42, respectively. T/NT in the group with mixed antibodies (group C) was evidently higher than those in the other two groups with

Table 5. In Vivo Distribution of ^{99m}Tc-CD44- mAb in Tumor-bearing Nude Mice (%ID/g, Mean ± SD, n=6)

	2h	4h	8h	16h	24h
Tumor	3.21±1.22	5.16±1.63	6.58±2.10	10.15±3.18[c]	7.77±2.84
Blood	6.45±2.37	5.38±2.26	4.35±1.82	3.01±1.53	2.82±1.21
Heart	5.78±2.36	3.86±2.20	2.78±1.51	1.91±0.86	1.33±0.49
Liver	8.85±3.81	7.12±3.15	5.22±2.54	4.45±1.71	3.41±1.32
Spleen	8.79±3.65	6.99±2.96	5.12±2.12	4.38±1.68	3.25±1.24
Lung	4.99±2.51	3.38±2.03	2.08±1.09	1.58±0.61	1.12±0.55
Kidney	5.12±2.78	10.15±4.01	5.68±2.92	3.49±2.16	2.66±1.15
Stomach	1.52±0.56	1.43±0.41	1.26±0.28	0.98±0.21	0.79±0.14
Bowel	1.41±0.40	1.30±0.31	1.18±0.26	0.97±0.18	0.71±0.11
Muscle	1.22±0.22	1.11±0.15	0.99±0.11	0.79±0.08	0.60±0.06
Bone	1.15±0.17	1.10±0.13	0.92±0.10	0.71±0.09	0.53±0.06
brain	0.91±0.11	0.80±0.08	0.72±0.06	0.61±0.05	0.46±0.03

Note: [c]: $p < 0.05$(compared to other four time point)

Table 6. Comparison of T/B, T/M at Time Point of 16h After Injection in Each Group (Mean ± SD, n=6)

	Group A	Group B	Group C
Tumor/blood	2.98±0.52	2.67±0.38	5.45±0.88[d]
Tumor/muscles	14.35±3.28	11.85±3.02	25.65±5.98[d]

Note: [d]: $p < 0.05$(compared to group A and group B)

single antibodies (groups A and B) ($p < 0.05$).

In vivo distribution of radiolabeled antibody for tumor-bearing nude mice

The in vivo radioactivity distribution of the three groups of nude mice bearing lung adenocarcinoma xenografts at each time point after injection of different radiolabeled antibodies are shown in Tables 3, 4, and 5. These tables show identical patterns of the in vivo distributions for each group. The uptake of the tumor was relatively low during the early stage, but increased gradually over time. The uptake reached its peak at 16 h post-injection. By contrast, the radioactivity uptake in the other tissues or organs gradually decreased with time, except that in the kidneys given that the imaging agent may be excreted through these organs. In addition, among the main organs, the radioactivity distribution was relatively high in the heart, liver, spleen, lung, and kidneys, but relatively low in the stomach, intestine, muscle, skeleton, and brain. The values of T/B and T/M at 16 h post-injection for each group are shown in Table 6. The values of T/B and T/M in group C (mixed antibodies) were evidently higher than those in the other two groups (single antibodies) ($p < 0.05$). These results suggest that the use of mixed antibodies can increase tumor uptake, compared with the single application of each antibody.

Discussion

Clinicians have applied in recent years all types of specific radiolabeled antibodies to tumor-specific expression antigens for diagnosis (RII) or therapy (radioimmunotherapy [RIT]) (Goldenberg et al., 2007). Some studies have achieved important progress in these fields, such as the use of specific radiolabeled mAb of alpha fetal protein (AFP) for the diagnosis and treatment of primary carcinoma of the liver (Shi et al., 1997). RII is an important molecular nuclear medicine imaging technology that may play an important role in the early diagnosis and specific localization of tumors.

Extensive animal experiments and clinical research for RII have been performed in non-small-cell lung cancer (NSCLC) in recent years (Kwa et al., 1996; Machac et al., 2002; Egri and Takáts, 2005; Goldenberg et al., 2006; Goldenberg et al., 2007). The United States has approved the clinical use of ^{99m}Tc-NR-LU-10 for the diagnosis of lung cancer using the RII kit (Rusch et al., 1993). However, generally speaking, there are only a few valuable achievements of RII in lung cancer primarily because of the lack of tumor-specific expressed antigens and the antigens with too weak antigenicity or heterogeneity in lung cancer. These factors result in the low uptake of radiolabeled antibodies (Ren et al., 2001). Hence, finding one or more tumor-specific highly expressed antigens and methods to increase the uptake of radioactivity at the tumor site is the key to the development of lung cancer RII.

EGFR is a type of glucoprotein receptor on the cell surface and is the expression product of proto-oncogene C-erb-1(HER-1). With protein tyrosine kinase (PTK) activity, this receptor is composed of four parts, namely, the extracellular region, transmembrane domain, intracellular region, and C terminal. The extracellular region is a ligand-binding region. The typical adenosine triphosphate (ATP) binding site and stenoplastic PTK region are contained in the cytomere. The PTK of the receptor is activated through the combination of ligands and EGFR. The signal transmission function of EGFR was also achieved by such combination. CD44 is another type of transmembrane protein in the family of adhesion molecules that exists widely on the cell surface. The biological functions of this protein include the activation of achroacyte, participation in signal transmission, and the facilitation of cell adhesion. Overexpression of these two transmenbrane proteins have been demonstrated in many studies, and they play important roles in facilitating the proliferation, invasion, metastasis, and apoptosis of lung cancer cells (Cichy et al., 2005; Malle et al., 2005; Gao et al., 2007; Sartori et al., 2007; Eren et al., 2008; Fukui and Mitsudomi, 2008; Hirsch et al., 2008; Ikeda et al., 2008; Jin et al., 2011). In the present study, these two membrane proteins were selected as antigens of lung adenocarcinoma. Their mAbs were radiolabeled with $^{99m}TcO_4^-$, and we obtained ideal radiolabeled mAbs with good physical properties, stability, and immunoreactivity. High uptakes of both radiolabeled mAbs at the tumor site have been demonstrated by RII and the in vivo distribution of nude mice bearing human lung adenocarcinoma xenografts. The results indicate that EGFR and CD44 may be ideal target antigens for human lung adenocarcinoma.

The lower uptake of the radiolabeled single antibodies at the tumor site is another critical factor that constrains the development of tumor RII or RIT. Weak antigenicity or heterogeneity of the tumor-specific antigens may cause the low uptake. RII may show a false negative in the tumor by the application of a single antibody. Several clinicians have tried to seek methods to increase the uptake of radiolabeled antibodies. Mixed radiolabeled antibody imaging (several mAbs of different tumor-specific antigens for the same tumor mixed for imaging after administration, namely, cocktail method of antibodies) may enhance the RII

target/non-target ratio in the present study (Hay et al., 2002; Petronzelli et al., 2005). Several studies have shown that the increase in tumor radioactive uptake was not significant with the double dosage of mAb, but it increased significantly with the combined application of mAb. In addition, the combined application of radiolabeled mAb showed a wider anticancer spectrum. The combined application may also increase the radioactivity and sensitivity uptake of the tumor in RII research. A mixture of radiolabeled mAb of EGFR and CD44 was applied in the present study, in which the radioactive uptake in the tumor was enhanced significantly by both biodistribution. The T/NT, T/B, and T/M of group C (mixed antibodies) were evidently higher than those of the other two groups (single antibodies) at 16 h post-injection ($p < 0.05$). These results indicate that the application of mixed antibodies should be the preferred mode in tumor RII to increase the radioactivity uptake of the tumor tissue.

In the present research, however, an identical pattern exists in the variation of RII and in vivo distribution study of each antibody and mixed antibodies. During the early stage (2 h to 4 h) of the intravenous injection of radiolabeled antibodies in each group, the radioactive background in blood was high and a significant uptake was found in some organs, such as the liver, spleen, lung, heart, in contrast to the tumor location which did not display good radioactivity. Possible reasons may include the following. First, the radiolabeled antibodies existed mainly in the blood during the early stage. The abundant blood supply in major organs, including the liver, spleen, and heart, resulted in the high radioactive distribution in these organs. Another reason may be the non-specificity in the uptake of organs, including that in the liver, spleen, and lung, of the radiolabeled antibody. Third, EGFR and CD44 are slightly expressed on the surface of these organs. With time, the radioactivity distribution in the blood and these organs declined gradually, whereas the radioactivity accumulation in the tumor location increased gradually. The radioactive uptake in the tumor location was highest at 16 h post-injection, with the best tumor stain in RII. Thus, the optimal time for RII should be 16 h post- injection of radiolabeled antibodies.

In summary, finding tumor-specific and high-expression antigens in the tissue of lung cancer is the key to RII. The application of mixed antibodies of different tumor-specific expression antigens can increase radioactivity uptake significantly, which is a highly necessary method in RII research for lung cancer.

Acknowledgements

This work was supported by the National Natural Science Foundation of China (2005, 30570523), and I thank very much to Professor André Constantinesco (MD, PhD, Service de Biophysique et Médecine Nucléaire, Hôpital de Hautepierre, France), who have offered many help and direction in the work and writing paper.

References

Artiko V, Petrović M, Sobić-Saranović D, et al (2011). Radioimmunoscintigraphy of colorectal carcinomas with ^{99m}Tc-labelled antibodies. *Hepatogastroenterology*, **58**, 347-51.

Bellomi M, Rampinelli C, Funicelli L, et al (2006). Screening for lung cancer. *Cancer Imaging*, **6**, 9-12.

Boswell CA, Brechbiel MW (2007). Development of radioimmunotherapeutic and diagnostic antibodies: an inside-out view. *Nucl Med Biol*, **34**, 757-78.

Cichy J, Kulig P, Puré E (2005). Regulation of the release and function of tumor cell-derived soluble CD44. *Biochim Biophys Acta*, **1745**, 59-64.

Egri G, Takáts A (2005). The immunodiagnosis of lung cancer with monoclonal antibodies. Med Sci Monit, 11, 296-300.

Eren B, Sar M, Oz B (2008). MMP-2, TIMP-2 and CD44v6 Expression in Non-small-cell Lung Carcinomas. *Ann Acad Med Singapore*, **37**, 32-9.

Fritzberg AR, Abrams PG, Beaumier PL, et al (1988). Specific and stable labeling of antibodies with technetium with a diamide dithiolate chelating agent. *Proc Natl Acad Sci USA*, **85**, 4025-9.

Fukui T, Mitsudomi T (2008). Mutations in the epidermal growth factor receptor gene and effects of EGFR-tyrosine kinase inhibitors on lung cancers. *Gen Thorac Cardiovasc Surg*, 56, 97-103.

Gao SP, Mark KG, Leslie K, et al (2007). Mutations in the EGFR kinase domain me-diates STAT3 activation via IL-6 production in human lung adenocarcinomas. *J Clin Invest*, **117**, 3846-56.

Gmeiner Stopar T, Fettich J, Zver S, et al (2008). ^{99m}Tc-labelled rituximab, a new non-Hodgkin's lymphoma imaging agent: first clinical experience. *Nucl Med Commun*, **29**, 1059-65.

Goldenberg DM, Chatal JF, Barbet J, et al (2007). Cancer imaging and therapy with bispecific antibody pretargeting. *Update Cancer Ther*, **2**, 19-31.

Goldenberg DM, Sharkey RM, Paganelli G, et al (2006). Antibody pretargeting advances cancer radioimmunodetection and radioimmunotherapy. *J Clin Oncol*, **24**, 823-34.

Granville CA, Dennis PA (2005). An overview of lung cancer genomics and proteomics. *Am J Respir Cell Mol Biol*, **32**, 169-76.

Greenlee RT, M urray T, Bolden S, et al (2000). Cancer statistics 2000. *CA Cancer J Clin*, **50**, 7-33.

Hay RV, Cao B, Skinner RS, et al (2002). Radioimmunoscintigraphy of tumors autocrine for human met and hepatocyte growth factor/scatter factor. *Mol Imaging*, **1**, 56-62.

Hirsch FR, Dziadziuszko R, Thatcher N, et al (2008.) Epidermal growth factor receptor immunohistochemistry;comparison of antibodies and cutoff points to predict benefit from gefitinib in a phase 3 placebo-controlled study in advanced nonsmall-cell lung cancer. *Cancer*, **112**, 1114-21.

Ikeda K, Nomori H, Mori T, et al (2008). Novel germline mutation: EGFR V843I in patient with multiple lung adenocarcinomas and family members with lung cancer. *Ann Thorac Surg*, **85**, 1430-2.

Jin Y, Li JP, Tang LY, et al (2011). Protein expression and significance of VEGF, EGFR and MMP-9 in non-small cell lung carcinomas. *Asian Pac J Cancer Prev*, **12**, 1473-6.

Kwa HB, Wesseling J, Verhoeven AH, et al (1996). Immunoscintigraphy of small-cell lung cancer xenografts with anti neural cell adhesion molecule monoclonal antibody, 123C3: improvement of tumour uptake by internalisation. *Br J Cancer*, **73**, 439-46.

Lopez AD (1998). Counting the dead in China: measuring tobacco's impact in the developing world. *BMJ*, **317**, 1399-400.

Machac J, Krynyckyi B, Kim C (2002). Peptide and antibody imaging in lung cancer. *Semin Nucl Med*, **32**, 276-92.

Malle D, Valeri RM, Phatiou C, et al (2005). Significance of immunocytochemical expression of E-cadherin, N-cadherin and CD44 in serous effusions using liquid-based cytology. *Acta Cytol*, **49**, 11-6.

Neal RD, Allgar VL, Ali N, et al (2007). Stage, survival and delays in lung, colorectal, prostate and ovarian cancer: comparison between diagnostic routes. *Br J Gen Pract*, **57**, 212-9.

Petronzelli F, Pelliccia A, Anastasi AM, et al (2005). Improved tumor targeting by combined use of two antitenascin antibodies. *Clin Cancer Res*, **11**, 7137-45.

Ren XL, Wang J, Jin BQ, et al (2001). Lung cancer radioimmunoimaging using 99Tcm-labeled anti-epidermal growth factor recepter monoclonal antibody in nude mice. *Chin J Nucl Med*, **21**, 28-9.

Rom WN, Hay JG, Lee TC, et al (2000). Molecular and genetic aspects of lung cancer. *Am J Respir Crit Care Med*, **16**, 1355-67.

Rusch V, Macapinlac H, Heelan R, et al (1993). NR-LU monoclonal antibody scanning. A helpful new adjunct to computed tomography in evaluating non-small-cell lung cancer. *J Thorac Cardiovasc Surg*, **106**, 200-4.

Sartori G, Bettelli S, Schirosi L, et al (2007). Microsatellite and EGFR, HER2 and K-RAS analyses in sclerosing hemangioma of the lung. *Am J Surg Pathol*, **31**, 1512-20.

Shi L, Wu M, Chen H (1997). Radioimmunologic targeting and therapy with antihuman primary hepatic cancer monoclonal antibodies (Hepama I) in patients. *Zhonghua Zhong Liu Za Zhi*, **19**, 146-9.

Smith-Jones PM, Pandit-Taskar N, Cao W, et al (2008). Preclinical radioimmunotargeting of folate receptor alpha using the monoclonal antibody conjugate DOTA-MORAb. *Nucl Med Biol*, **35**, 343-51.

Tachfouti N, Belkacemi Y, Raherison C, et al (2012). First data on direct costs of lung cancer management in Morocco. *Asian Pac J Cancer Prev*, **35**, 1813-5.